# Designing yeast as plant-like hyperaccumulators for heavy metals

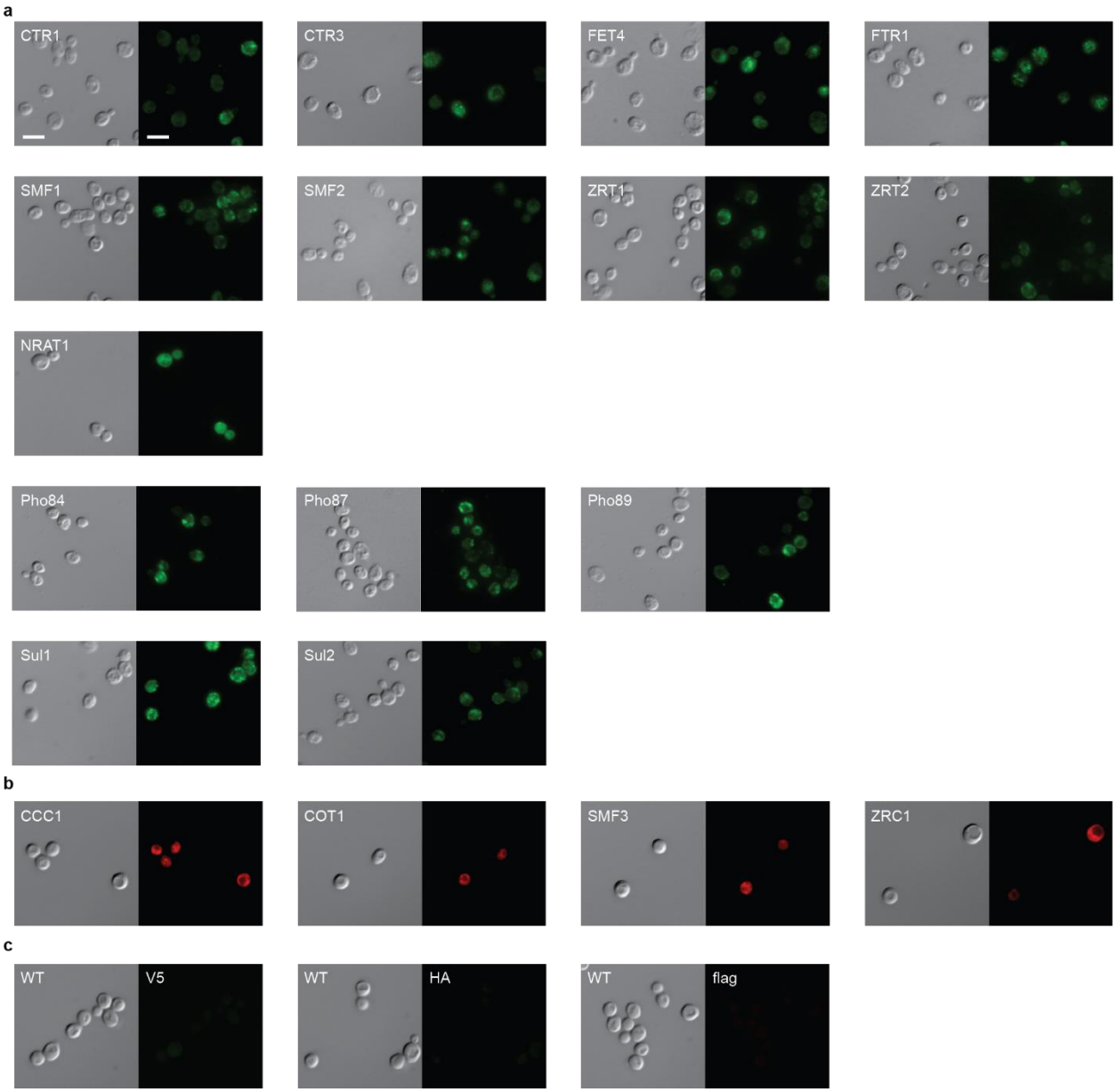


**Supplementary Figure 1. Visualization of fluorescently stained membrane and vacuole transporters. a**) Membrane transporters CTR1, CTR3, FET4, FTR1, SMF1, SMF2, ZRT1, ZRT2 and Nrat1 were fused with a C'-terminus V5 tag and stained. Pho84, Pho87, Pho89, and Sul1 and Sul2 were fused with a C'-terminus HA tag and stained. **b**) Vacuole transporters CCC1, COT1, SMF3, and ZRC1 were fused with a C'-terminus flag tag and stained. **c**) Negative controls of WT were stained with identical antibodies targeting V5, HA, and flag tag in parallel

with the transporters already described. No noticeable background fluorescence was observed. All tags were labelled with the appropriate primary and secondary antibodies conjugated with either an Alex488 (green; membrane) or Alex647(far red; vacuole) dye. Scale bars represent 5 $\mu$m for all images.

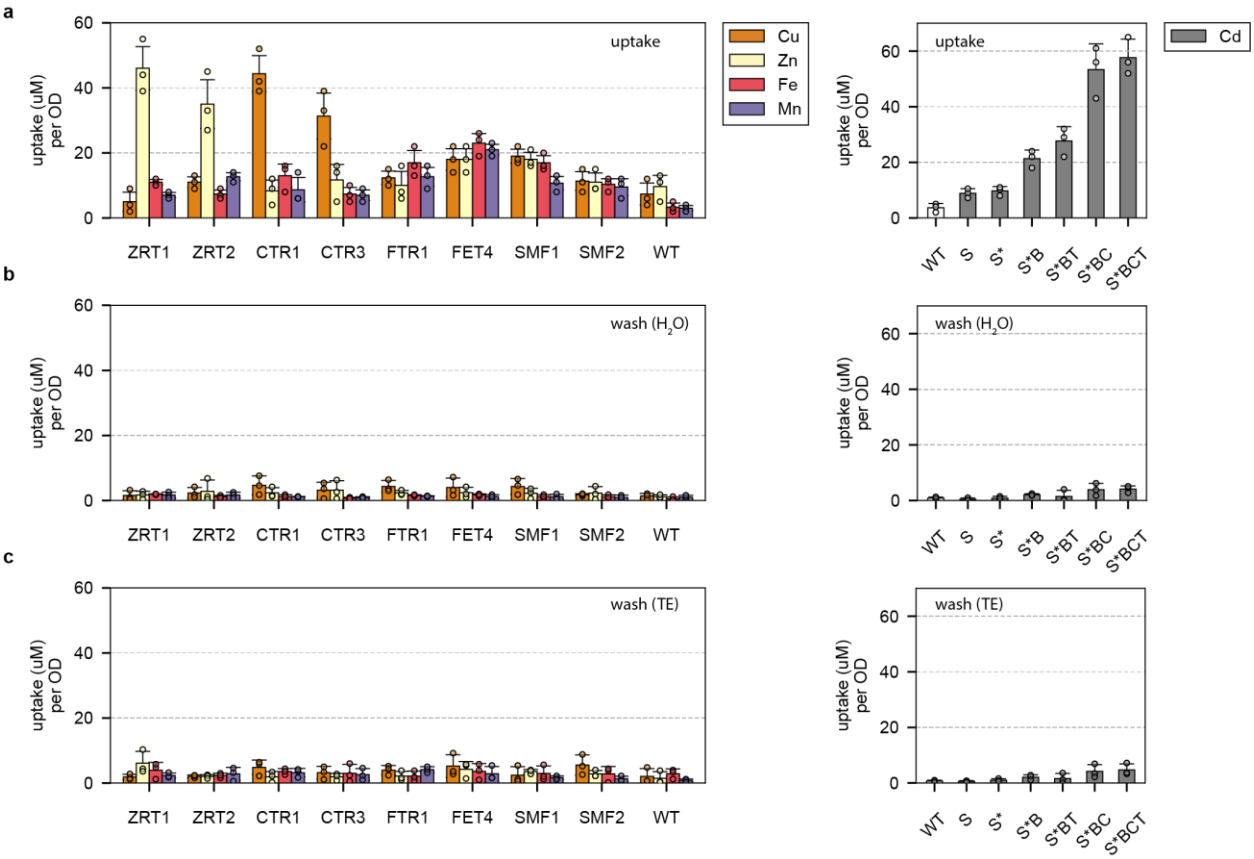


**Supplementary Figure 2. Impact of non-specific metal binding during metal uptake experiments. a**) Measurement of metal removed from a 100 $\mu$M metal uptake experiment (refer to Figure 1b and 3a). **b**) After a metal uptake experiment, cells were washed with dd$H_2O$ and supernatant measured for freed metal. **c**) After the dd$H_2O$ wash step, another wash step in a 1 mM EDTA buffer was similarly measured for freed metal. For all data, the mean $\pm$ s.d. of three replicates are shown.

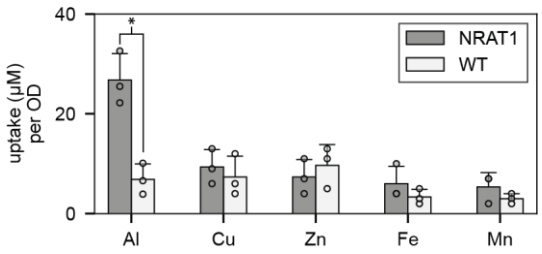


**Supplementary Figure 3. Nrat1 uptake is selective for $Al^{3+}$ ions.** Metal uptake experiments for Nrat1 was performed with Al, Cu, Zn, Fe, and Mn and compared against a non-expressing WT strain. Asterisk above bar chart represents significant uptake when compared to WT ($p < .05$). For all data, the mean $\pm$ s.d. of three replicates are shown.

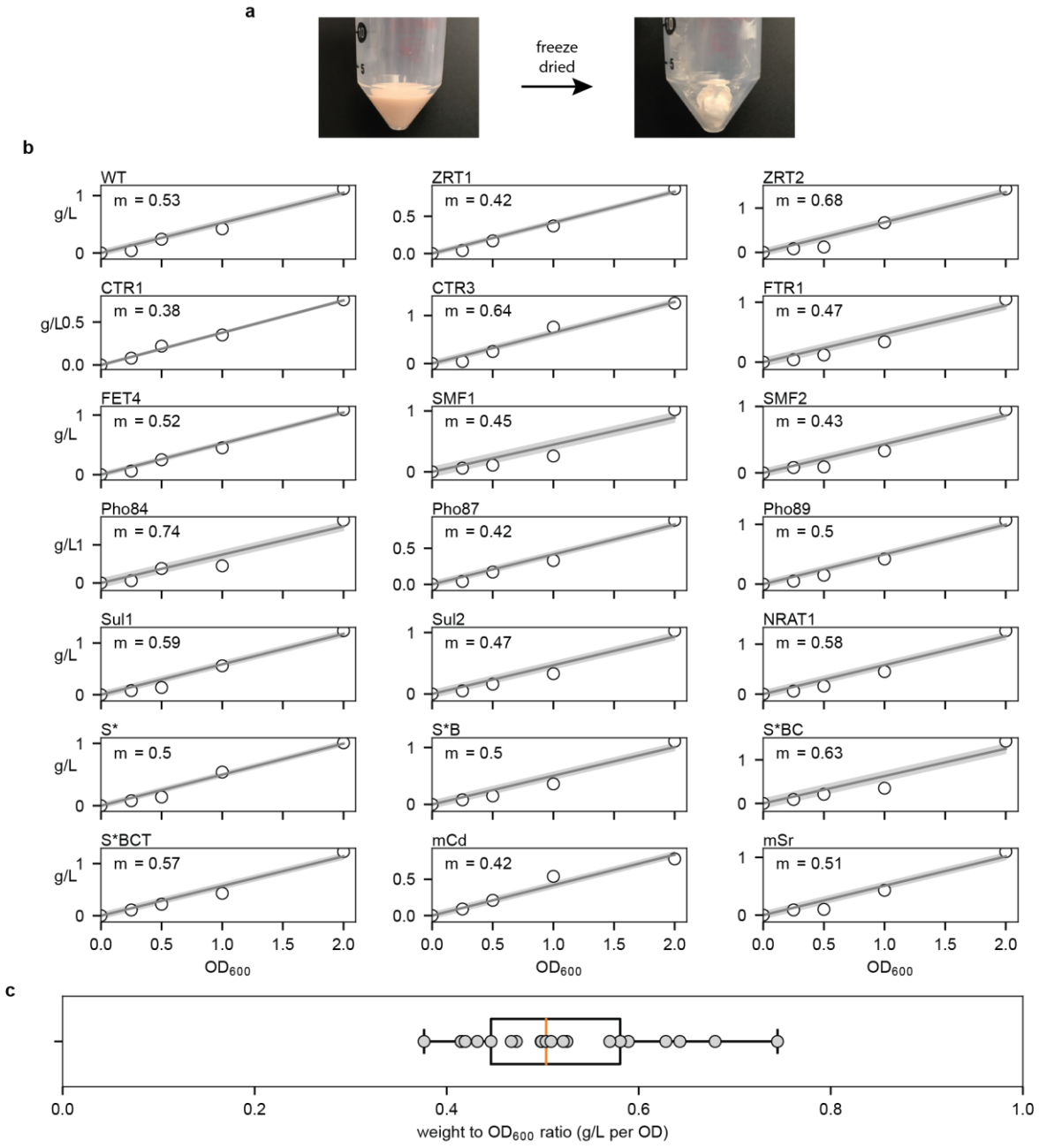


**Supplementary Figure 4. Correlating culture optical density ($OD_{600}$) to grams of culture dry weight. a**) Cells were grown, washed, pelleted, and freeze-dried to obtain culture dry weight per culture volume. Masses were weighed on a precision scale with hundredths of milligram resolution. **b**) A line of best fit with intercept at 0 was performed to obtain a correlation factor between optical density ($OD_{600}$) and gram of dry weight (gDW) per culture volume for each

strain. **c**) A box plot of all $OD_{600}$ to gram dry weight correlation factors. On average the correlation factor was approximately 0.52 g/L per $OD_{600}$. For all data, the mean ± s.d. of three replicates are shown.

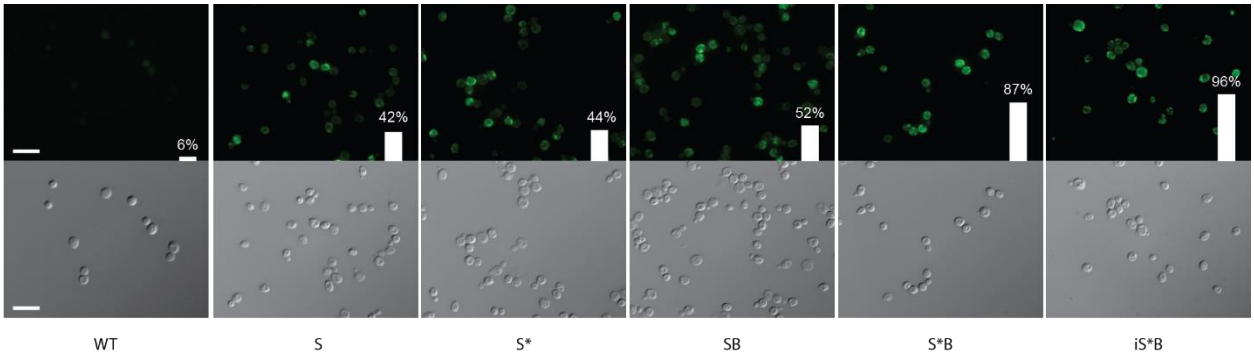


**Supplementary Figure 5. Increasing SMF1 expression with increased modifications.** Labels from left to right: WT, overexpression of SMF1 (S), SMF1 with K33,34R mutation (S*), S with BSD2 deletion (SB), S* with BSD2 deletion (S*B), and S integrated with BSD2 deletion (iS*B). Bars and values indicate percent expression after subtracting background signal from WT controls. Images and expression scores were calculated using ImageJ. Scale bars represent 10 $\mu$m for all images.

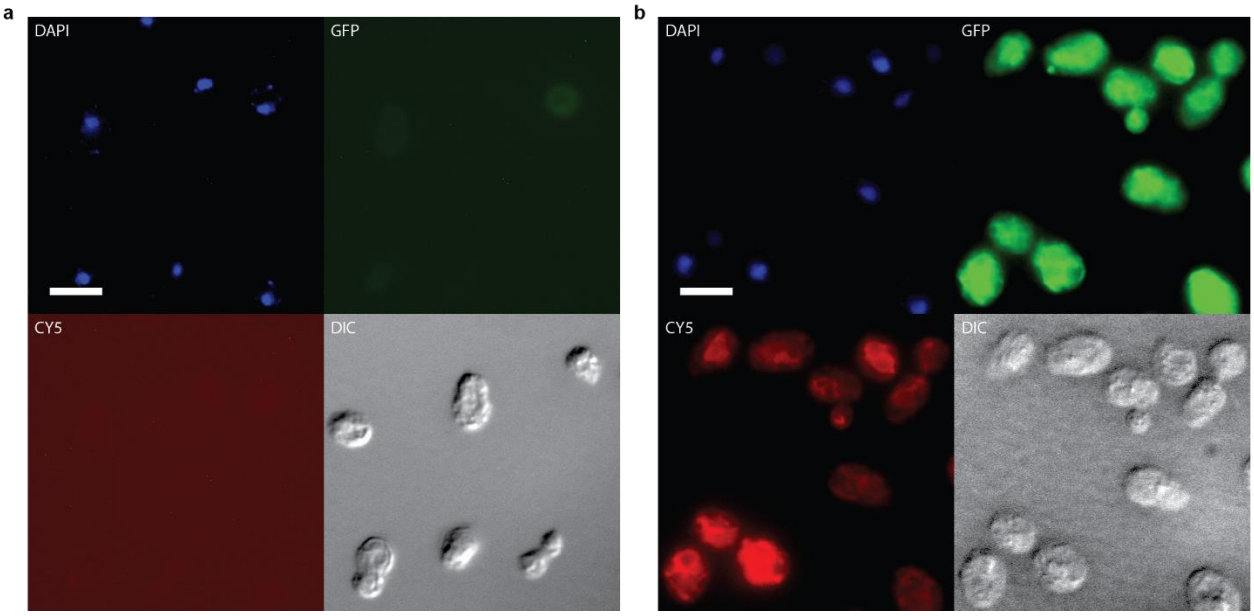


**Supplementary Figure 6. Visualization of fluorescently labelled co-expression of SMF1 and CCC1. a**) Fluorescent measurements of non-expressing WT strain as a control. **b**) SMF1* was fused with a C' terminus V5 tag, whereas CCC1 was fused with a C' terminus flag tag. Tags were stained with the appropriate primary and secondary antibodies conjugated with either an Alex488 (green; SMF1*) or Alex647(far red; CCC1) dye, respectively. Scale bars represent 5 $\mu$m for all images.

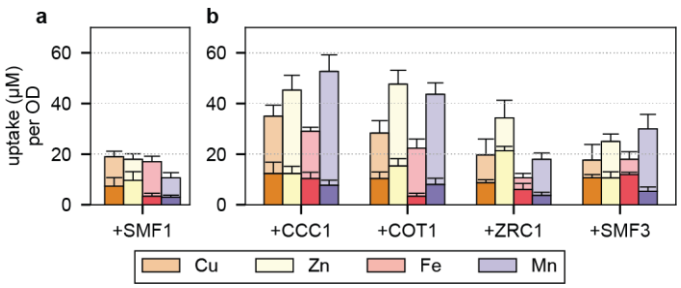


**Supplementary Figure 7. Increasing metal uptake with the addition of a vacuole transporter. a**) Heavier colored bars represent WT metal uptake. Lighter colored overlaid bars represent metal uptake with SMF1 expression (S; no modifications). **b**) Heavier colored bars represent metal uptake with vacuole transporter expression. Lighter colored overlaid bars represent metal uptake with co-expression of SMF1. For all data, the mean ± s.d. of three replicates are shown.

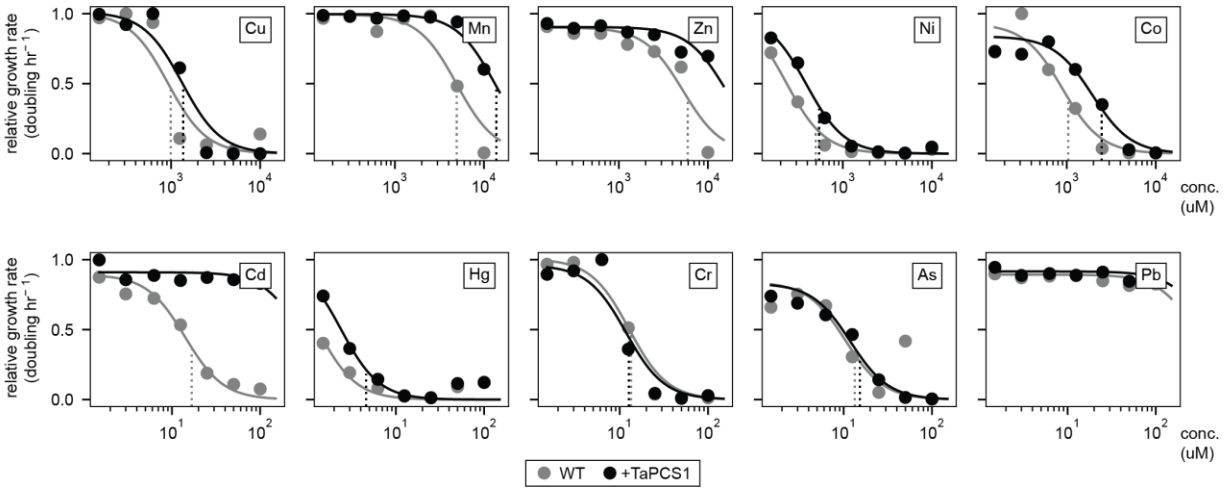


**Supplementary Figure 8. TaPCS1 improves metal tolerance for a variety of transition metals.** Cu, Mn, Zn, Ni, and Co were added to cultures from 10 $\mu$M to 10 mM. Cd, Hg, Cr, As, and Pb were added to cultures from 1 $\mu$M to 100 $\mu$M. The addition of TaPCS1 slightly enhanced tolerance to Cu, Mn, Zn and Co in the millimolar range. Of the more toxic elements, TaPCS1 specifically conferred tolerance to Cd while changing little against Hg, Cr, and As. Growth rate curves for Pb and Fe were misleading as Fe and Pb precipitated in culture during the 24-hour growth experiment. For all data, the growth rates were fitted with growth curves of three replicates.

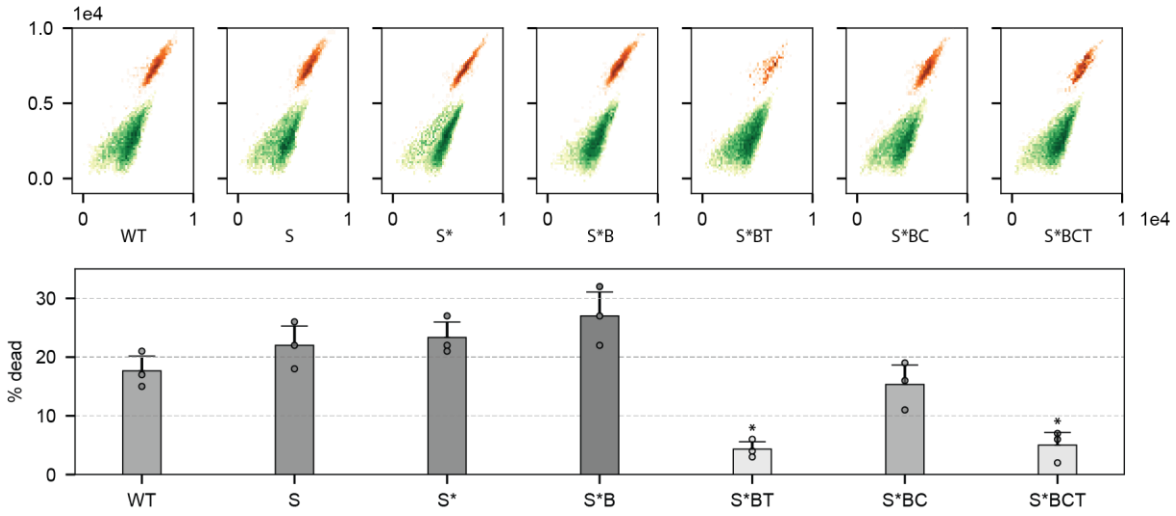


**Supplementary Figure 9. Percent survival after metal uptake experiments measured by FACS live-dead assay.** Increased transporter expression (**Supplementary Figure 5**) and cadmium uptake (**Figure 2a**) loosely correlated to increase cell death during metal uptake experiments (WT → S → S* → S*B). Expression of TaPCS1 (T) and CCC1 (C) enhanced cell viability despite increased cadmium uptake. Asterisk above bar charts represent significance change in survival percentage ($p < .05$) compared to WT. For all data, the mean ± s.d. of three replicates are shown.

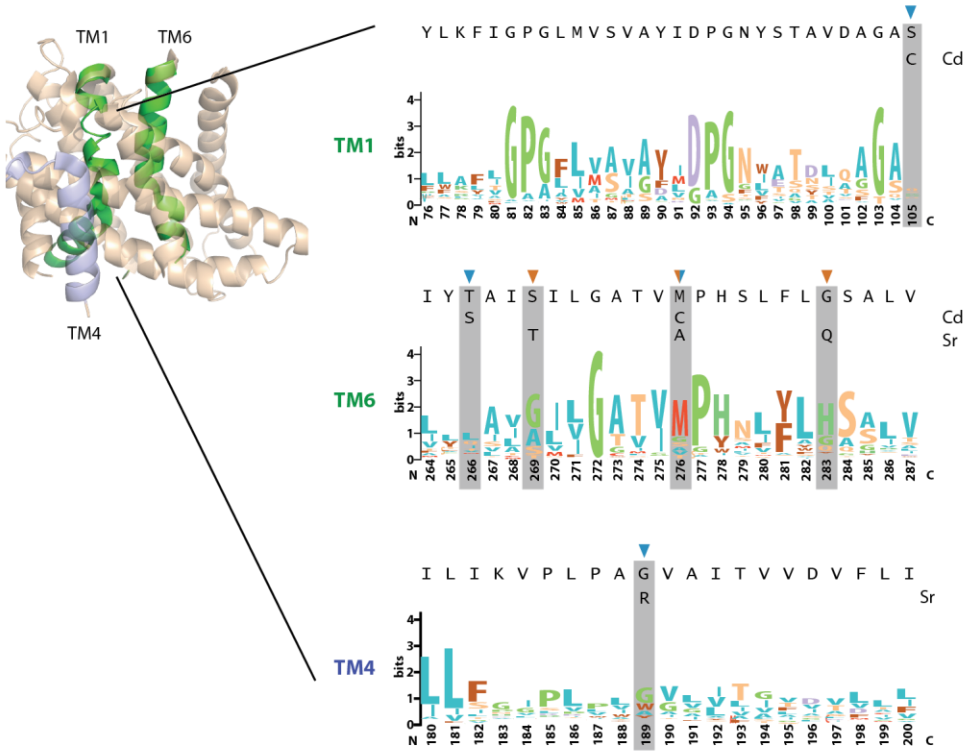


**Supplementary Figure 10. Mutations in transmembrane regions TM1 and 6 (green) and TM4 (blue).** Mutations introduced based on previous findings[34] were M276C for cadmium mutants, and G189R and M276A for strontium mutants. Mutations discovered using the developed transporter assay were S105C and T266S for cadmium mutant mCd, and S269T and G283Q for mSr.

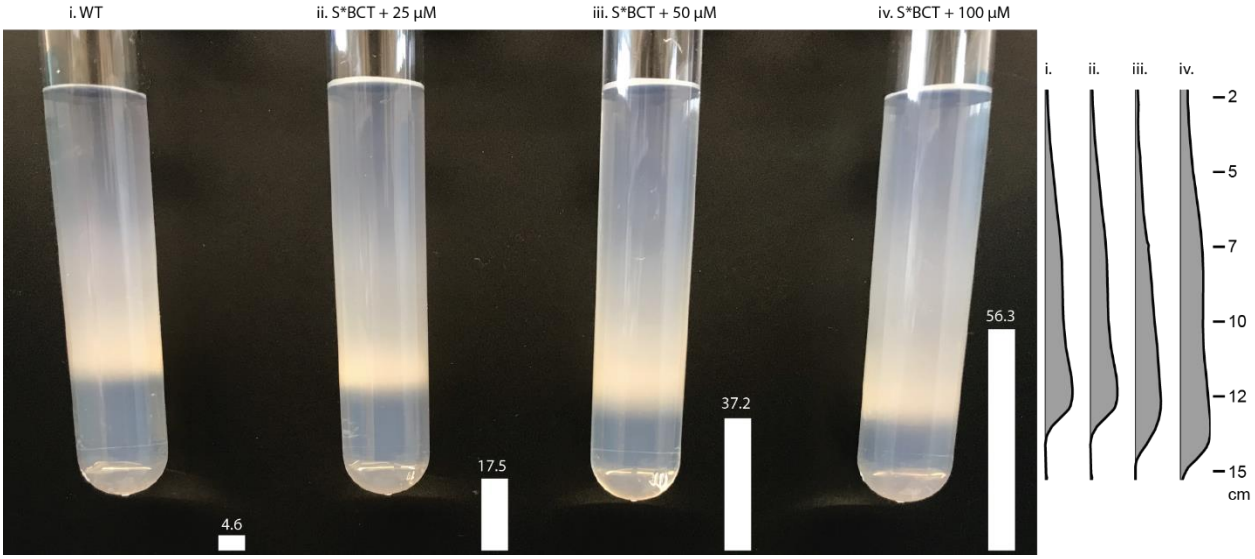


**Supplementary Figure 11. Fractionating cells based on metal uptake using rate-zonal density gradient centrifugation.** Conditions from left to right were: (i) WT incubated with 100 $\mu$M cadmium; (ii), (iii), and (iv) S*BCT strain incubated with 25, 50, and 100 $\mu$M cadmium, respectively. Bottom bar charts indicate the amount of metal uptake per condition. Left chart shows the population distribution of migrated cells by measuring the tube's opacity as a function of height using ImageJ. Ticks represent distance measured from the meniscus to the tube's bottom in centimeters.

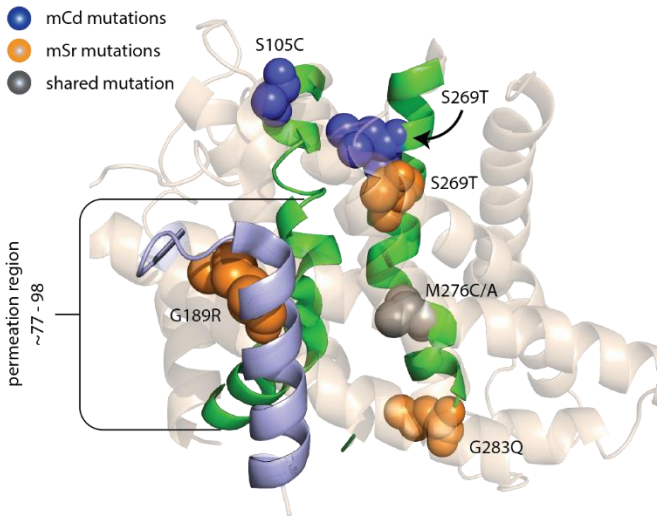


**Supplementary Figure 12. Approximate mutation locations for mCd and mSr on homologue DraNramp (PDB 5KTE).** Many of the mutations for both mCd and mSr reside on TM6, or at the entry of TM1. This could suggest that the region 77-98 (41-61 for DraNramp) in the first alpha-helix sequence of TM1 is highly sensitive to mutations, as observed in previous works[33,35,36]. This region, referred to as the permeation region[33], has a highly conserved DPGN sequence which may act as an actuator to transport metals through the inner cavity. Whereas, TM6 and 4 may provide the spacing and environment to select for certain metals.

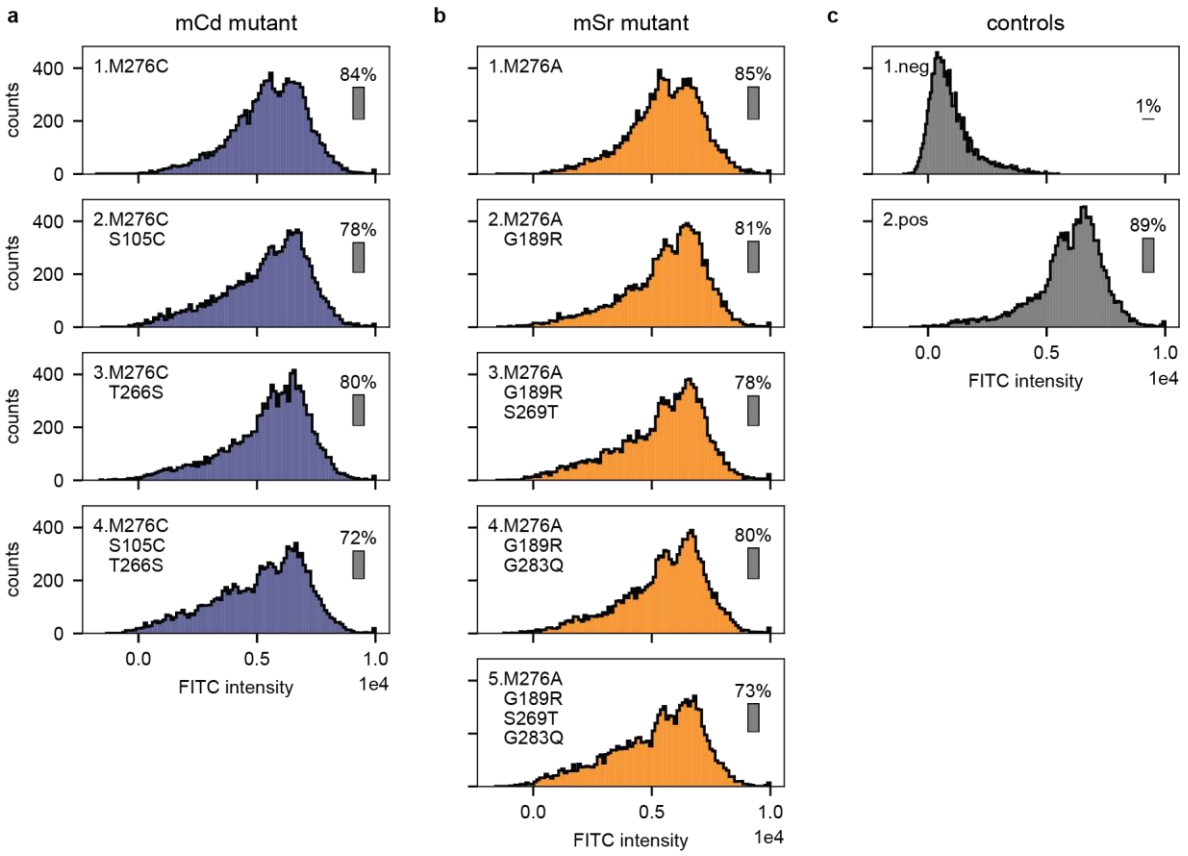


**Supplementary Figure 13. Effect of mCd and mSr mutations on SMF1 expression. a**) Mutants were fluorescently labelled and measured using flow cytometry. Progressive mutations (1-4; corresponding to numberings in **Figure 5b**) leading to mCd caused little change in transporter expression. **b**) Likewise, a slight reduction in mSr transporter expression was observed, but not significant. **c**) Negative (WT) and positive controls (S*BCT) were also measured to compare expression changes with non-engineered strains.

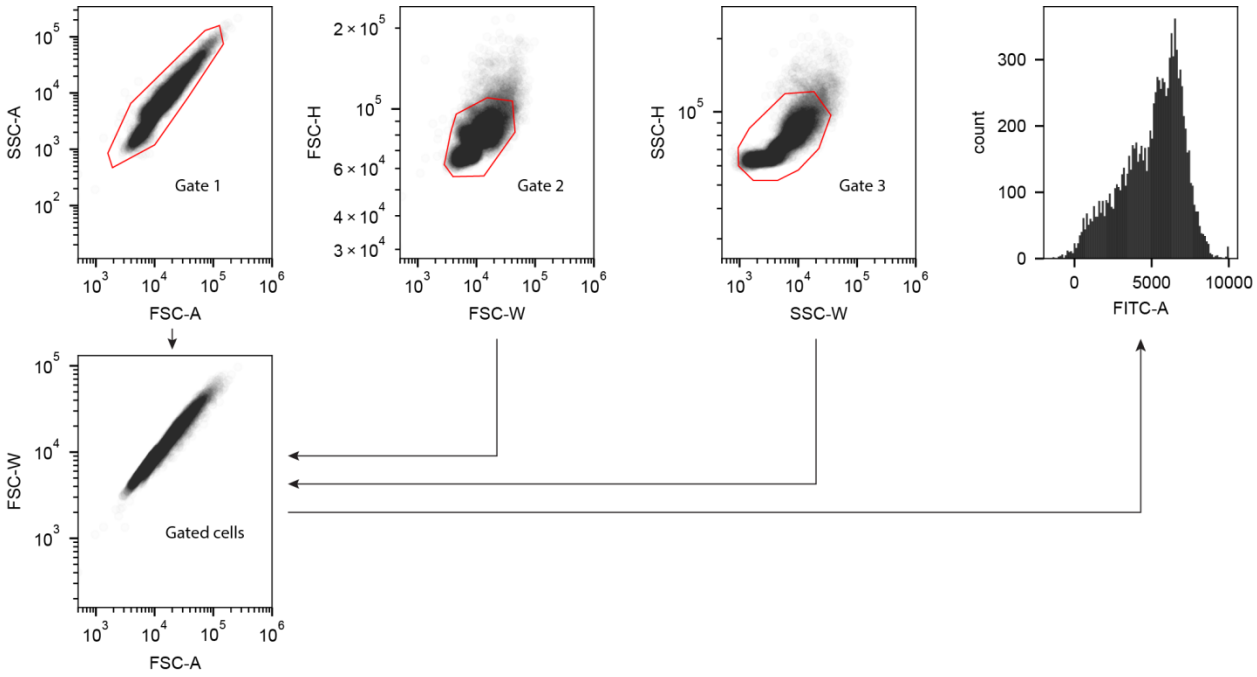


**Supplementary Figure 14. Yeast gating strategy for flow cytometry measurements**. FSC-A and SSC-A gated cells. FSC-W and FSC-H gated vertically oriented cells (vertical singlets). SSC-W and SSC-H gated horizontally oriented cells (horizontal singlets). Gating on these 3 plots, single cells were measured for fluorescence.

**Supplementary Table 1. Hyperaccumulator values for engineered strains.**

| strain | metal | uptake (μM) | uptake (mg/g) | hyper threshold (mg/g) |
|---|---|---|---|---|
| ZRT1 | Zn | 46 ± 6.7 | 7.3 ± 1.1 | 10 |
| ZRT2 | Zn | 35 ± 7.5 | 3.4 ± 0.7 | 10 |
| CTR1 | Cu | 44 ± 5.6 | 7.5 ± 0.9 | 1 |
| CTR3 | Cu | 31 ± 7.0 | 3.1 ± 0.7 | 1 |
| FTR1 | Fe | 17 ± 3.7 | 2.0 ± 0.4 | 10 |
| FET4 | Fe | 23 ± 2.9 | 2.5 ± 0.3 | 10 |
| SMF1 | Mn | 11 ± 2.1 | 1.3 ± 0.3 | 10 |
| SMF2 | Mn | 10 ± 2.6 | 1.2 ± 0.3 | 10 |
| Pho84 | As | 28 ± 3.8 | 2.8 ± 0.4 | 0.1 |
| Pho87 | As | 13 ± 1.0 | 2.4 ± 0.2 | 0.1 |
| Pho89 | As | 18 ± 3.0 | 2.8 ± 0.5 | 0.1 |
| Sul1 | Cr | 25 ± 2.4 | 2.2 ± 0.2 | 1 |
| Sul2 | Cr | 24 ± 1.9 | 2.7 ± 0.2 | 1 |
| NRAT1 | Al | 27 ± 4.3 | 1.2 ± 0.2 | 1 |
| S* | Cd | 10 ± 1.3 | 2.2 ± 0.3 | 0.1 |
| S*B | Cd | 21 ± 2.5 | 4.8 ± 0.6 | 0.1 |
| S*BC | Cd | 53 ± 7.6 | 9.5 ± 1.4 | 0.1 |
| S*BCT | Cd | 58 ± 5.4 | 11.4 ± 1.1 | 0.1 |
| S*BCT | Mn | 328 ± 14.8 | 31.7 ± 1.4 | 10 |
| mCd | Cd | 43 ± 4.6 | 11.5 ± 1.2 | 0.1 |
| mSr | Sr | 30 ± 3.9 | 5.1 ± 0.7 | N/A |

Transporters and strains developed in this work that are within or have exceeded the hyperaccumulating thresholds[12,13] for their respective metal.

**Supplementary Table 2. Divalent metal transporter primers for pYES2/CT subcloning.**

| name | direction | sequence |
|---|---|---|
| ZRT1 | fwd | TAAGCAGGTACCATGAGCAACGTTACTACG |
| | rev | TAAGCACTCGAGAGCCCACTTACCGATC |
| ZTR3 | fwd | TAAGCAGGTACCATGGAAAAAATTCCCAGGTG |
| | rev | TAAGCACTCGAGAGTGAAAAGGGCACTC |
| CTR1 | fwd | TAAGCAGGTACCATGGAAGGTATGAATATGG |
| | rev | TAAGCACTCGAGGTTATGAGTGAATTTTTCG |
| CTR3 | fwd | TAAGCAGGTACCATGAATATGGGAGGCAG |
| | rev | TAAGCACTCGAGCAAGCAGCATTTGC |
| FET4 | fwd | TAAGCAGGTACCATGGGTAAAATTGCAGAG |
| | rev | TAAGCACTCGAGTTTTTCCAACATCATAACC |
| FTR1 | fwd | TAAGCAGGTACCATGCCTAACAAAGT |
| | rev | TAAGCACTCGAGAAGAGAGTCGGCTTTAAC |
| SMF1 | fwd | TAAGCAGGTACCATGGTGAACGTTGG |
| | rev | TAAGCACTCGAGACTGATATCACCATGAGAC |
| SMF2 | fwd | TAAGCAGGTACCATGACGTCCCAAGAATAT |
| | rev | TAAGCACTCGAGGAGGTGTACTTCTTTGC |

Cloning strategy involved amplifying the appropriate regions and using the KpnI and XhoI restriction sites**.**

**Supplementary Table 3. Permease primers for pYES2/CT subcloning.**

| name | direction | sequence |
|---|---|---|
| Sul1 | fwd | ATAGGGAATATTAAGCTTGGTACCGAGCTCATGTCACGTAAGAGCTC |
| | rev | AGCGTAGTCTGGAACGTCGTATGGGTAGGATCCACCGCCAACGTCCCATTTAGAAAAATC |
| Sul2 | fwd | ATAGGGAATATTAAGCTTGGTACCGAGCTCATGTCCAGGGAAGGTTA |
| | rev | AGCGTAGTCTGGAACGTCGTATGGGTAGGATCCACCGCCGATATCCCATTTAGCAAAATC |
| Pho84 | fwd | ATAGGGAATATTAAGCTTGGTACCGAGCTCATGAGTTCCGTCAATAAAGATAC |
| | rev | AGCGTAGTCTGGAACGTCGTATGGGTAGGATCCACCGCCTGCTTCATGTTGAAGTTGAG |
| Pho87 | fwd | ATAGGGAATATTAAGCTTGGTACCGAGCTCATGAGATTCTCACACTTTCTCA |
| | rev | AGCGTAGTCTGGAACGTCGTATGGGTAGGATCCACCGCCAGTGCTACCTTTTAAGACG |
| Pho89 | fwd | ATAGGGAATATTAAGCTTGGTACCGAGCTCATGGCTTTACATCAATTTGACT |
| | rev | AGCGTAGTCTGGAACGTCGTATGGGTAGGATCCACCGCCTGTCATTTGGTATTCCACAC |
| pYES2/CT | fwd | GAGCTCGGTACCAAGCTTAATATTC |
| | rev | GGCGGTGGATCCTACCCATACGACGTTCCAGACTACGCTTAAGTTTAAACCCGCTGATCC |

Cloning strategy also involved substituting the V5 tag by appending primers with the HA tag.

**Supplementary Table 4. Nrat1 primers for pYES2/CT subcloning.**

| name | direction | sequence |
|---|---|---|
| NRAT1 | fwd | CTCACTATAGGGAATATTAAGCTTGGTACCATGGAAGGTACTGGTGAAATG |
| | rev | ACCGAGGAGAGGGTTAGGGATAGGCTTACCCATACTAGCATCTGCCAAATCTT |
| pYES2/CT | fwd | GGTAAGCCTATCCCTAACCC |
| | rev | GGTACCAAGCTTAATATTCCCTATAGTG |

Nrat1 was first codon-optimized from *O. sativa* and synthesized from Genscript before amplifying and assembling into pYES2/CT.

**Supplementary Table 5. Vacuole transporter primers for modified pYES2/CT subcloning.**

| name | direction | sequence |
|---|---|---|
| CCC1 | fwd | GTCTTAGAGCTCGTCTTAGAGCTCATGTCCATTGTAGCACTAAAGA |
| | rev | GTCTTAGGATCCTTAACCCAGTAACTTAACAAAGAAC |
| COT1 | fwd | ATAGGGAATATTAAGCTTGGTACCGAGCTCATGAAACTCGGAAGCAA |
| | rev | ATCCTTGTAATCACTTCCACCTCCGGATCCATGATCCTCTAAGCAATCAG |
| ZRC1 | fwd | ATAGGGAATATTAAGCTTGGTACCGAGCTCATGATCACCGGTAAAGAATTG |
| | rev | ATCCTTGTAATCACTTCCACCTCCGGATCCCAGGCAATTGGAAGTATTGC |
| SMF3 | fwd | ATAGGGAATATTAAGCTTGGTACCGAGCTCATGCGATCTTATATGCAGATTC |
| | rev | ATCCTTGTAATCACTTCCACCTCCGGATCCAAAATGGATGTCGGCAC |

The pYES2/CT vector was modified to contain the LEU marker instead of its URA marker. CCC1 was first cloned via SacI and BamHI restriction enzymes, and later modified to contain a downstream flag tag instead of the V5 tag. COT1, ZRC1, and SMF3 were amplified with PCR and Gibson assembled into the modified pYES2/CT vector replacing CCC1.

**Supplementary Table 6. Primers used to construct S*BCT strain.**

| name | direction | sequence |
|---|---|---|
| SMF1* | fwd | TCAATTACCACTGTAGAATCTCTCCTATCCCTCAGTTCGAATACTTCTTC |
| | rev | GAAGAAGTATTCGAACTGAGGGATAGGAGAGATTCTACAGTGGTAATTGA |
| ΔBSD2::HIS | fwd | TGAGAATAACAAGAACACGTAGTCTAGGAAACTAAGCGCTTATTACTCTTGGCCTCCT |
| | rev | AAAGTTATATATCTCTTTTTATCATAATGAAGAAGATGGCCCTGATGCGGTATTTTCT |
| TaPCS1 | fwd | CTAAGGGGATGGAGGCTCTT |
| | rev | ATGGAGGTGGCGTCG |
| pD1235 | fwd | CACCCGCCGGTACAGCGACGCCACCTCCATTTTATCCGTCGAAACTAAG |
| | rev | GAGGCATGTCAAGAGCCTCCATCCCCTTAGCAGGTTAAATCATGTAATTAGTTATG |
| iTaPCS1 | fwd | CACCCGCACGGCAGAGACCAATCAGTAAAAATCAACGGTTTCATTATCAATACTCGCCAT |
| | rev | CAAGTGCACAAACAATACTT |
| part1-GAL | fwd | CAGTCACGACGTTGTAAAACGACGGCCAGTAGTACGGATTAGAAGCCG |
| | rev | GGTTTTTTCTCCTTGACGT |
| part2-CCC1 | fwd | AGTTTCGACGGATTCTAGAACTAGTGGATCCTCATGTCCATTGTAGCACTA |
| | rev | GCAGCTTGCAAATTAAAGC |
| part3-LEU | fwd | GACGCTCGAAGGCTTTAATTTGCAAGCTGCAACTGTGGGAATACTCAGG |
| | rev | CACGTTGAGCCATTAGTATC |
| part4-pUC18 | fwd | TACCTCTATACTTTAACGTCAAGGAGAAAAAACCGTCATAGCTGTTTCCTGTGT |
| | rev | ACTGGCCGTCGTTTTA |
| iCCC1 | fwd | AACTGTGGGAATACTCAGGTATCGTAAGATGCAAGAGTTCAGTACGGATTAGAAGCCG |
| | rev | CACGTTGAGCCATTAGTATC |

SMF1* was created using mutagenesis primers altering the K33,34 region (*AAGAAA*) into arginines (*AGGAGA*). ΔBSD2 was created by replacing the BSD2 gene with the HIS3 cassette amplified from pRS303. TaPCS1 was constitutively integrated into the genome by replacing the TRP auxotrophic marker of W303$\alpha$. The GAL1 inducible CCC1 construct was assembled using Gibson assembly, and product was genomically integrated into the genome.

**Supplementary Table 7. Library generation and site-directed mutagenesis primers for SMF1*.**

| name | direction | sequence |
|---|---|---|
| mTM1 | fwd | GCAGGTAATGAGAGATATTTTTGCTAAA |
| | rev | CAAAATGATACAAAGTAGGGAAAATTGATT |
| mTM6 | fwd | CCAAATGTTTGACCACAATGGT |
| | rev | GTCATAATCTAAAAGCCTTGGCTG |
| Cd-S105C | fwd | GTCGATGCAGGTGCCTGTAATCAATTTTCCCTAC |
| Cd-T266S | fwd | CCAAATGTTTGACCACAATGGTATTTATTCTGCTATTTCCATCTTAGGTGC |
| Cd-M276C | fwd | CTATTTCCATCTTAGGTGCTACTGTTTGTCCACATTCGTTGTTTTTGGGTTCC |
| Sr-G189R | fwd | GTGCCCCTTCCAGCGAGAGTGGCCATTACTGTT |
| Sr-S269T | fwd | GACCACAATGGTATTTATACCGCTATTACTATCTTAGGTGCTACTGTTA |
| Sr-M276A | fwd | CTATTTCCATCTTAGGTGCTACTGTTGCTCCACATTCGTTGTTTTTGGGTTCC |
| Sr-G283Q | fwd | GTTATGCCACATTCGTTGTTTTTGCAATCCGCTTTAGTGCAGCCAA |

Primers used to error-prone PCR regions TM1 and 6 of SMF1 to construct libraries using Agilent's GeneMorph(II) protocol. Afterwards, site-directed mutagenesis primers were used to selectively mutate residues identified to have effects on SMF1 metal preference and uptake.